Title

Androgen receptor transcriptional activity is required for heregulin-1β—mediated nuclear localization of the HER3/ErbB3 receptor tyrosine kinase

Journal

Journal of Biological Chemistry, 299(8)

ISSN

0021-9258

Authors

Jathal, Maitreyee K

Siddiqui, Salma

Vasilatis, Demitria M

et al.

Publication Date

2023-08-01

DOI

10.1016/j.jbc.2023.104973

Peer reviewed

JBC RESEARCH ARTICLE

Androgen receptor transcriptional activity is required for heregulin-1β–mediated nuclear localization of the HER3/ErbB3 receptor tyrosine kinase

Received for publication, November 16, 2022, and in revised form, June 5, 2023 Published, Papers in Press, June 26, 2023,
https://doi.org/10.1016/j.jbc.2023.104973

Maitreyee K. Jathal[1,2], Salma Siddiqui[1], Demitria M. Vasilatis[1,3], Blythe P. Durbin Johnson[4], Christiana Drake[5], Benjamin A. Mooso[1], Leandro S. D'Abronzo[3], Neelu Batra[6], Maria Mudryj[1,2], and Paramita M. Ghosh[1,3,6,*]

From the [1]Research Service, VA Northern California Health Care System, Mather, California, USA; [2]Department of Medical Microbiology and Immunology, University of California Davis, Davis, California, USA; [3]Department of Urologic Surgery, University of California Davis, Sacramento, California, USA; [4]Division of Biostatistics, Department of Public Health Sciences, and [5]Department of Statistics, University of California Davis, Davis, California, USA; [6]Department of Biochemistry and Molecular Medicine, University of California Davis, Sacramento, California, USA

Reviewed by members of the JBC Editorial Board. Edited by Eric Fearon

Prostate cancer is initially regulated by the androgen receptor (AR), a ligand-activated, transcription factor, and is in a hormone-dependent state (hormone-sensitive prostate cancer (HSPC)), but eventually becomes androgen-refractory (castration-resistant prostate cancer (CRPC)) because of mechanisms that bypass the AR, including by activation of ErbB3, a member of the epidermal growth factor receptor family. ErbB3 is synthesized in the cytoplasm and transported to the plasma membrane for ligand binding and dimerization, where it regulates downstream signaling, but nuclear forms are reported. Here, we demonstrate in prostatectomy samples that ErbB3 nuclear localization is observed in malignant, but not benign prostate, and that cytoplasmic (but not nuclear) ErbB3 correlated positively with AR expression but negatively with AR transcriptional activity. In support of the latter, androgen depletion upregulated cytoplasmic, but not nuclear ErbB3, while *in vivo* studies showed that castration suppressed ErbB3 nuclear localization in HSPC, but not CRPC tumors. *In vitro* treatment with the ErbB3 ligand heregulin-1β (HRG) induced ErbB3 nuclear localization, which was androgen-regulated in HSPC but not in CRPC. In turn, HRG upregulated AR transcriptional activity in CRPC but not in HSPC cells. Positive correlation between ErbB3 and AR expression was demonstrated in AR-null PC-3 cells where stable transfection of AR restored HRG-induced ErbB3 nuclear transport, while AR knockdown in LNCaP reduced cytoplasmic ErbB3. Mutations of ErbB3's kinase domain did not affect its localization but was responsible for cell viability in CRPC cells. Taken together, we conclude that AR expression regulated ErbB3 expression, its transcriptional activity suppressed ErbB3 nuclear translocation, and HRG binding to ErbB3 promoted it.

The androgen receptor (AR) is a ligand-activated, nuclear steroid hormone receptor which regulates prostate development and homeostasis and modulates cell function *via* transcriptional regulation of target genes (1). Prostate cancer (PCa) arises from aberrant AR signaling, and the AR target gene prostate-specific antigen (PSA) is often used as a marker of PCa progression. Due to the strong involvement of the AR in PCa development, the first line of treatment for disseminated PCa (beyond localized PCa) is usually androgen deprivation therapy, ADT, alone or together with AR inhibition (1). While initially effective, PCa tumors eventually become refractory to ADT and are termed "castration-resistant prostate cancer" (CRPC) (1). CRPC tumors no longer respond to AR inhibition but may continue to express high levels of AR mRNA and protein and retain its transcriptional activity.

Multiple causes have been attributed to the development of CRPC, including AR amplification and mutations, alterations in AR coregulators, altered steroidogenesis, the development of AR splice variants, and the aberrant activation of alternative pathways that regulate prostate cell growth (2). The AR consists of an N-terminal domain, followed by a DNA-binding domain (DBD), a hinge region, and a C-terminal ligand-binding domain (LBD). AR splice variants that induce resistance to ADT typically lack the AR-LBD (1). Another cause for treatment resistance is aberrant receptor tyrosine kinase (RTK) activation, for example, the activation of the epidermal growth factor receptor (EGFR) family whose members EGFR, ErbB2, ErbB3, and ErbB4 are implicated in tumor development and progression (3, 4). These receptors are typically localized in the plasma membrane but nuclear variants for full-length EGFR (5), ErbB2 (6) and nuclear localization of ErbB3 (7, 8) and ErbB4 (9) have been reported in normal tissues where they influence mechanisms of cell proliferation, survival, and differentiation *via* the mitogen-activated protein kinase/ERK and the PI3K/AKT pathways (9). ErbB3 is unique among the RTKs of the EGFR family because it contains a weak kinase domain and relies on dimerization with other RTKs for kinase activity (10). The kinase domain of ErbB3, however, has six binding sites for the PI3K regulatory subunit p85 that enables signaling to Akt (10).

* For correspondence: Paramita M. Ghosh, paghosh@ucdavis.edu.

Nuclear EGFR and ErbB2 are associated with increased aggressiveness and grade of various tumors (11, 12). Nuclear ErbB3 has been observed in and reported to be transcriptionally active in cancers of the breast (13, 14), lung (15), and prostate (16–18). In prostate tumors, nuclear ErbB3 discriminates normal from malignant prostate tissues, hormone-sensitive PCa (HSPC) *versus* hormone-refractory PCa, and is associated with risk of disease progression (16, 17). Nuclear ErbB3 (full-length) is seen in primary tumors from patients who have undergone ADT (19) and predicts biochemical recurrence, following radical prostatectomy (16, 17). In addition to the full-length nuclear form, low-molecular-weight forms of ErbB3 have also been identified in PCa cells, where a 45-kDa form was secreted into the circulation (20). ErbB3 nuclear staining was predominantly an 80-kDa isoform matching the C-terminus domain of the full-length 185-kDa receptor (18); however, in breast cancer patients, this isoform has also been shown to be secreted into the circulation (21).

We have previously shown that ErbB3 levels increase as prostate tumors progress from benign to malignant to metastatic and this is associated with a loss of AR-mediated negative regulation (22). Here we used human prostatectomy specimens, animal models of HSPC and CRPC, as well as HSPC (LNCaP) and CRPC cell lines (C4-2, 22Rv1, PC3, PC3-wt-AR) to investigate the subcellular localization of ErbB3 and whether the AR regulated the nuclear form of this receptor. Our data suggest that the subcellular location and possible regulatory role of ErbB3 on the AR is altered once tumors achieve castration resistance.

Results

Nuclear ErbB3 is expressed mostly in PCa but not in benign prostate tissue

We investigated the expression of ErbB3 in primary prostate tumor and surrounding nontumor tissues of 78 patients with localized PCa previously described (23, 24). Prostatectomy tissue microarrays (TMAs) representing benign and malignant prostates were stained with an ErbB3 antibody directed toward the C-terminal portion of the receptor (Fig. 1*A*). Epithelial cells in tumor tissue as well as nontumor prostate stained for cytoplasmic ErbB3 and are significantly higher in the cytoplasm of cancer cells than in the cytoplasm of noncancer cells ($p < 0.001$), in support of our previous findings (22) (Fig. 1*B*). Higher magnification photomicrographs revealed the presence of nuclear ErbB3 in malignant tissue, but there is a notable absence of nuclear ErbB3 in most nontumor tissue (n < 1.0 in 56/70(80%), $p = 0.008$) (Fig. 1*B*). ErbB3 levels were higher in the cytoplasm than the nucleus in both tumor (median values: cytoplasm, 1.0; nucleus, 0.6; $p = 0.0003$) and nontumor (median values: cytoplasm, 0.5; nucleus, 0; $p = 0.0003$) tissue. ErbB3 staining in the cancer cells decreased with increased preoperative PSA (Spearman's rho = −0.25), although the correlation was marginally significant (Fig. 1*C*). Despite this, there was a significant positive correlation between cytoplasmic ErbB3 and nuclear (active) AR in the tumors (Spearman's rho = 0.32; $p = 0.013$) (Fig. 1*D*). Notably, no such correlation was observed between nuclear ErbB3 and nuclear AR (Spearman's Rho = −0.2; $p = 0.114$). Taken together, this indicates that AR expression is needed for ErbB3 protein expression, whereas its transcriptional activity regulates ErbB3 localization.

ErbB3 translocates to the nucleus in the presence of both androgens and HRG, and its expression is negatively correlated with PSA, but not AR, in HSPC LNCaP cells

Previous reports indicated that nuclear ErbB3 localization was induced by heregulin-1β (HRG) in breast cancer cells (13), and in PCa, it appeared to be affected by ADT (19). Here, we investigated whether HRG affected ErbB3 localization in PCa. We cultured HSPC LNCaP cells in media containing fetal bovine serum (FBS), which contain adequate levels of both steroids such as androgens (25) and growth factors such as HRG (26), or in charcoal-stripped serum (CSS) that lack both. The cells were also supplemented with 1 nM dihydrotestosterone (DHT), to activate AR, or 50 ng/ml HRG to activate ErbB3. In FBS, DHT increased nuclear AR levels but had negligible effect on PSA or ErbB3 levels or localization (supporting the discordance between AR expression and transcriptional activity noted above) (Fig. 2*A*) (densitometry analysis of nuclear and cytoplasmic ErbB3 and AR levels reported in Fig. 2, *B* and *C*). In contrast, HRG added to FBS increased ErbB3 and AR levels (compared to FBS control) but decreased PSA levels. Remarkably, both nuclear and cytoplasmic ErbB3 was upregulated in HRG-treated FBS-cultured cells (unlike culture in CSS, where only cytoplasmic ErbB3 was increased).

We previously showed that culture in CSS increased ErbB3 levels in LNCaP cells without evaluating the cellular compartment in which it was expressed (22, 27). We now report that, in support of the negative correlation between PSA and cytoplasmic ErbB3 reported in Figure 1*C*, in LNCaP cells, culture in CSS, which decreased PSA levels, increased ErbB3 expression in the cytoplasm (C-ErbB3) (Fig. 2, *A* and *B*). AR levels simultaneously increased (likely as a compensatory mechanism) when the cells were cultured in CSS (Fig. 2, *A* and *C*), in support of positive correlation between cytoplasmic ErbB3 and AR reported in Figure 1*D*. These effects were prevented by DHT, but not HRG, indicating a clear role for AR in controlling cytoplasmic (but not nuclear) ErbB3 expression, AR, and PSA levels. Cytoplasmic localization of ErbB3 was validated by colocalization of ErbB3 with calnexin, which is exclusively cytoplasmic (Fig. S1). Immunofluorescent microscopy supported the observation that ErbB3 was predominantly cytoplasmic in control cells (clear blue nuclei); however, HRG caused an increase in nuclear ErbB3 (illustrated by light blue nuclei indicative of the presence of green ErbB3 staining in the nuclear region) (Fig. 2*D*).

Culture in CSS also caused AR accumulation in the cytoplasm (indicating transcriptionally inactive AR), and this effect too was reversed only by DHT not HRG. AR transcriptional activity was measured by reporter gene assay on a PSA promoter (Fig. 2*E*). Treatment with DHT, but not with HRG, significantly increased AR transcriptional activity in FBS-treated cells ($p < 0.01$) (Fig. 2*E*), indicating discrepancy with

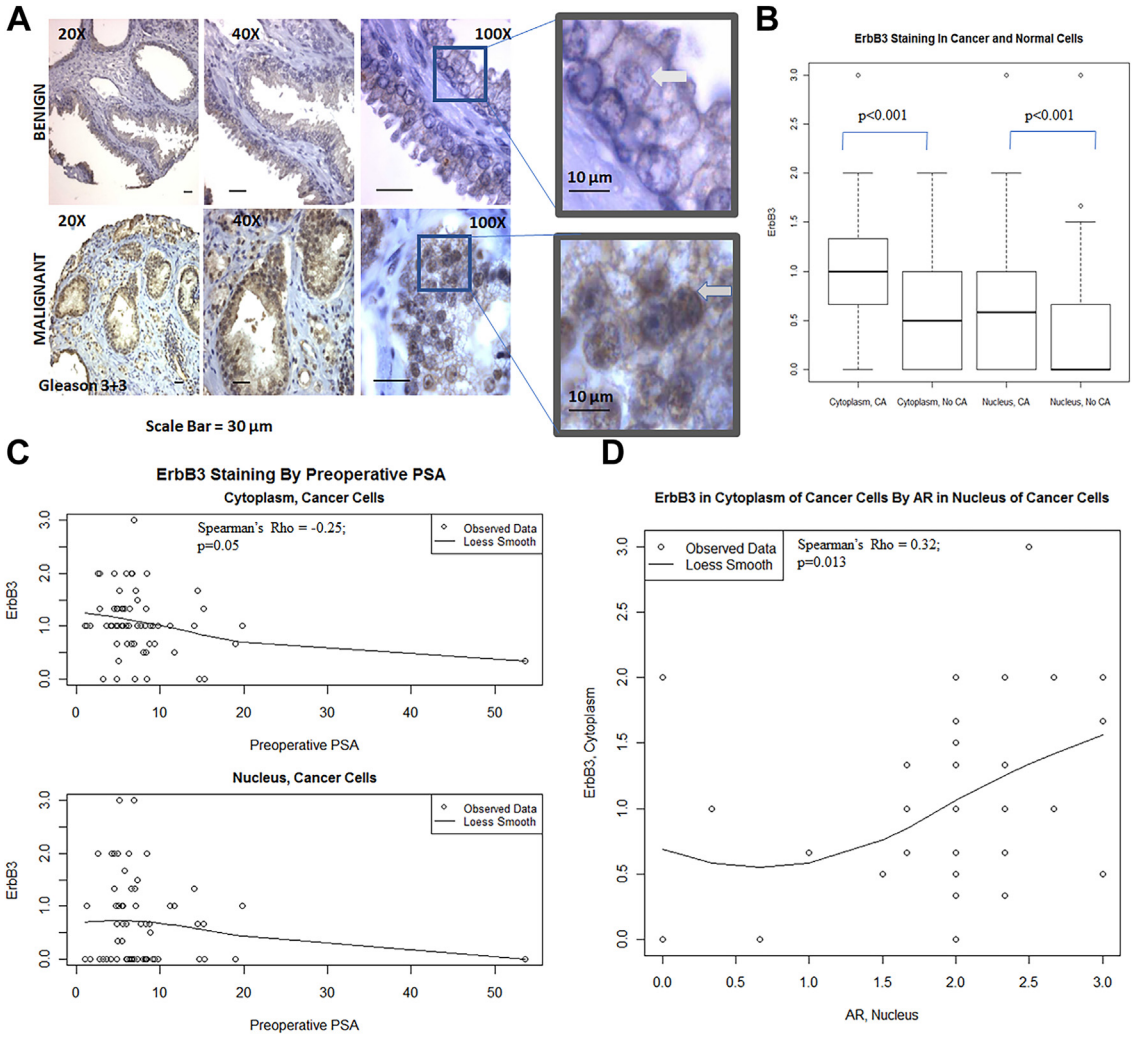

Figure 1. Expression of ErbB3 in the nucleus is exclusively seen in malignant, but not benign, prostate epithelia and correlates with AR expression but not that of AR target genes. *A*, prostatectomy samples from tumor and nontumor sections of the prostates of 78 patients were laid out in a tissue microarray (TMA) and sections from the TMA stained with anti-ErbB3 (C-terminal, kinase domain) antibody. ErbB3 stained exclusively the epithelial cells with no staining in the stroma. Bar represents the length of an epithelial cell at 20×, 40×, and 100× magnification. *Upper panel*: sections containing no tumor tissue (benign) showed ErbB3 expression exclusively in the cytoplasm. *Lower panel*: sections containing tumor tissue (malignant) expressed higher cytoplasmic ErbB3 but in addition, also showed nuclear localization of ErbB3. *B*, boxplot demonstrating median levels of ErbB3 in the cytoplasmic and nuclear compartments of tumor and nontumor sections. *C*, *upper panel*: negative correlation between cytoplasmic ErbB3 in the cancer cells and preprostatectomy PSA (p = 0.049, Spearman's rho = −0.25). *Lower panel*: no correlation between nuclear ErbB3 in the cancer cells and preprostatectomy PSA. *D*, positive correlation between cytoplasmic ErbB3 in the cancer cells and nuclear AR expression (Spearman's rho = 0.32; p = 0.013). AR, androgen receptor; PSA, prostate-specific antigen.

PSA protein levels reported in Figure 2*A* (which may be caused by rapid PSA degradation by nuclear ErbB3). On the other hand, AR transcriptional activity decreased in CSS ($p < 0.01$) but could be partially restored by DHT, but not by HRG, which is consistent with PSA protein levels. In FBS, HRG, but not DHT, increased Akt and Erk phosphorylation (pAkt and pERK, respectively). In contrast, culture in CSS did not have a significant effect on pAkt or pERK, although HRG stimulation caused a larger increase in ERK phosphorylation in CSS than in FBS. These results indicated that ErbB3 signaling, but not AR signaling, regulated Akt and ERK phosphorylation in LNCaP cells.

Next, we investigated the effects of HRG on ErbB3 phosphorylation. A major phosphorylation site on ErbB3 is Y1289, which is one of the six sites for binding of the PI3K regulatory subunit p85 (10). ErbB3 phosphorylation at Y1289 increased over time when the cells were cultured in FBS but remained steady when the cells were cultured in CSS, indicating that additional factors are required for regulation of ErbB3 phosphorylation by HRG (Fig. S2*A*). Accordingly, Akt phosphorylation also increased over time in FBS-treated cells. However, in CSS, Akt phosphorylation transiently increased but then subsided, indicating the need for other factors to sustain HRG-induced activation downstream of ErbB3 phosphorylation. The transient nature of AR transcriptional activity, seen in Fig. S2*B*, is likely responsible for this transient activation. Taken together, these results demonstrate that upon androgen deprivation, AR expression increases, thereby also increasing ErbB3 levels. Newly synthesized ErbB3 is translocated to the nucleus in LNCaP cells in the presence of androgens when

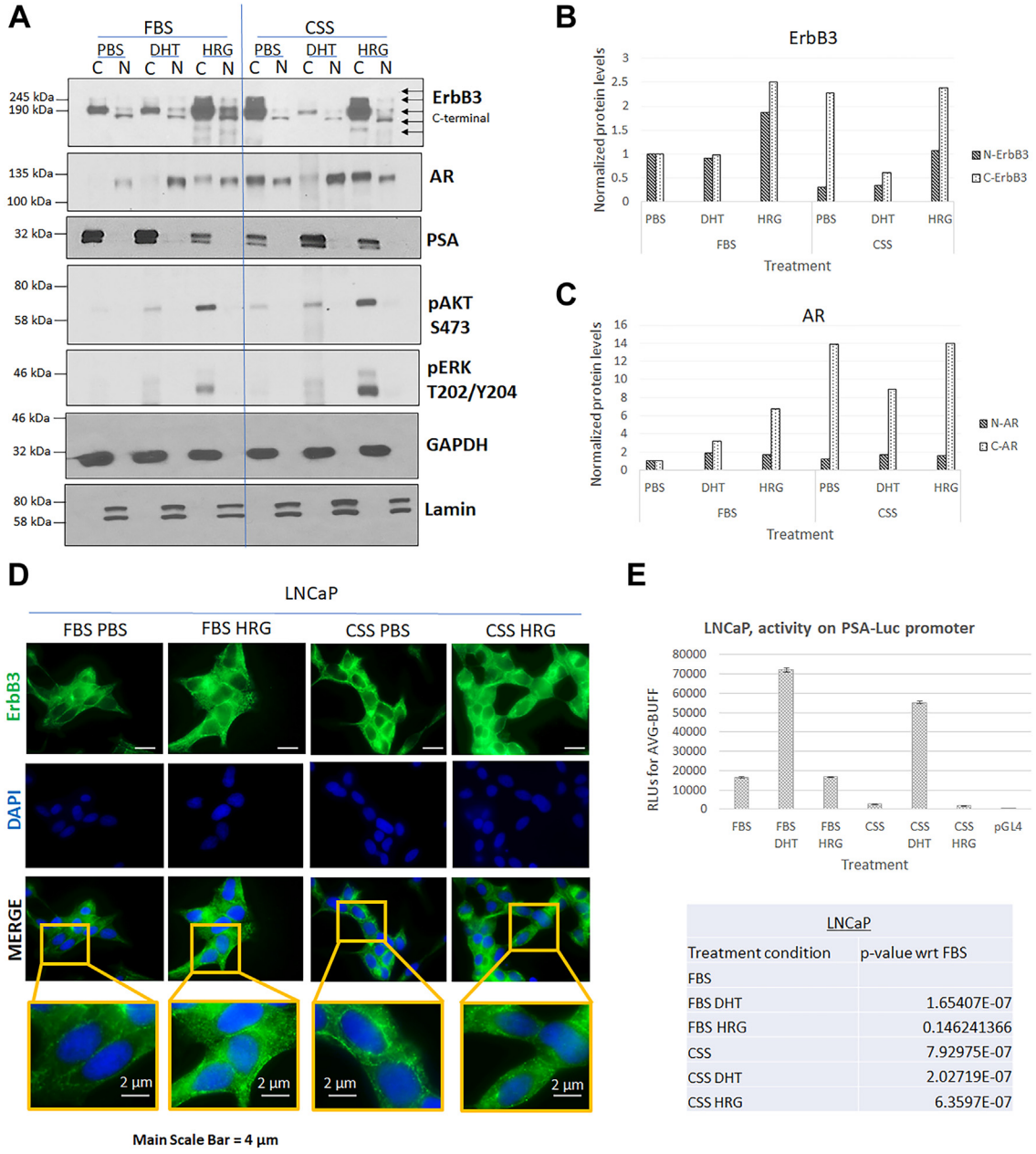

LNCaP	
Treatment condition	p-value wrt FBS
FBS	
FBS DHT	1.65407E-07
FBS HRG	0.146241366
CSS	7.92975E-07
CSS DHT	2.02719E-07
CSS HRG	6.3597E-07

Figure 2. HRG treatment, but not DHT, in LNCaP cells cultured in FBS, but not CSS, causes ErbB3 nuclear translocation. LNCaP cells were cultured in complete media (containing growth factors, steroid hormones, FBS, etc) or media lacking those constituents (CSS) for 72 h with or without ligands specific to activating the androgen receptor (AR) or ErbB3. Dihydrotestosterone (DHT, 1 nM, dissolved in 200-proof ethanol, EtOH) and heregulin-1β (HRG, dissolved in sterile PBS) were used to activate AR and ErbB3, respectively. Cells were separated into cytoplasmic and nuclear fractions and probed with antibodies to AR, ErbB3, and its downstream targets phosphorylated AKT and phosphorylated ERK. Twenty micrograms of protein lysates were loaded in each lane. Lamin and GAPDH were used as protein loading controls for crude nuclear and cytoplasmic fractions, respectively. *B*, quantitation of ErbB3 bands in the nucleus (N-ErbB3) and the cytoplasm (C-ErbB3). *C*, quantitation of AR band in the nucleus (N-AR) and the cytoplasm (C-AR). *D*, high-magnification microscopy showing the cytoplasmic localization of ErbB3 and an increase in ErbB3 protein when treated with HRG for 72 h. Cells were grown on coverslips and fixed for 10 min at room temperature with 100% ice-cold methanol before being incubated with ErbB3-specific antibodies approved for immunofluorescence. The scale bars represent 4 µm. *E*, LNCaP cells display increased AR transcriptional activity on a human PSA promoter when cultured with 1 nM DHT despite decreased viability, and this effect persists regardless of the presence of androgens. HRG treatment decreases AR transcriptional activity in the presence and absence of androgens. The PSA promoter sequence was housed in a pGL4 backbone (Promega). Promoter activity was recorded for individual samples using relative luminescent units. The results are from experiments performed in triplicate. Error bars represent SD from the mean. Table below shows *p*-values with respect to FBS alone. CSS, charcoal-stripped serum; FBS, fetal bovine serum; PSA, prostate-specific antigen.

treated with HRG but that also suppresses PSA protein levels, but not AR transcriptional activity on a PSA promoter, likely indicating posttranscriptional modifications that result in PSA degradation and explain the negative correlation between PSA and ErbB3, despite positive correlation between AR and ErbB3.

HRG is necessary for ErbB3 nuclear localization and an increase in AR transcriptional activity on a PSA promoter construct in CRPC C4-2 cells

C4 cells were derived by subcutaneous co-implantation of hormone-sensitive LNCaP cells with a bone marrow stromal

cell line into castrated adult male mice (28). C4-2 cells were derived from a chimeric tumor induced by co-inoculating castrated mouse with C4 cells and marrow stromal cells and are considered to be fully castration-resistant (28). ErbB3 typically signals from the plasma membrane (10); hence we compared ErbB3 localization to the plasma membrane by colocalization of ErbB3 with the membrane-localized protein E-cadherin in LNCaP and C4-2 cells (Fig. S3). ErbB3 appeared to be cytoplasmic and membrane localized in both LNCaP and C4-2 cells, but the proportion of membrane-bound ErbB3 in C4-2 cells was greater than that in LNCaP. In C4-2 cells, like in LNCaP, AR was mainly nuclear, especially in FBS, but partially translocated to the cytoplasm upon culture in CSS (Fig. 3*A*). Unlike in LNCaP cells, where 72 h treatment with HRG induced cytoplasmic AR localization, in C4-2 cells, HRG treatment restored AR nuclear localization. ErbB3 staining was predominantly plasma membrane–bound in untreated C4-2 cells cultured in FBS, whereas in HRG treatment, there was partial localization to the nucleus; but this effect was not seen when the cells were cultured in CSS (Fig. 3*A*).

Next, we investigated whether this difference in response to AR was caused by a difference in AR transcriptional activity. We have previously seen that in LNCaP cells, AR transcriptional activity as measured by reporter gene activity on a PSA promoter construct was decreased (though not significantly) by HRG (Fig. 2*E*). Treatment with DHT significantly increased AR transcriptional activity in C4-2 cell lines ($p < 0.01$), indicating an increase in AR transcriptional activity on the PSA promoter. However, when treated with HRG, in C4-2 cells, HRG increased AR transcriptional activity in FBS ($p < 0.01$) (Fig. 3*B*). As in LNCaP cells, CSS culture decreased AR transcriptional activity in C4-2 cells, and this effect was rescued by DHT but not by HRG. Thus, in C4-2 cells, unlike in LNCaP, HRG was able to increase AR transcriptional activity in the presence of androgens.

Castration prevents ErbB3 nuclear translocation in HSPC lines but not in CRPC lines

We next investigated whether HRG-induced ErbB3 nuclear localization in FBS-cultured cells is an artefact of LNCaP cells and related cells only. Since LNCaP and C4-2 are related, a second castration-resistant cell line, CWR22-Rv1 ("22Rv1"), which is derived from the CWR22 tumor line in castrated mice (29), was similarly treated with DHT and HRG, following prolonged culture in FBS or CSS. In these cells, ErbB3 protein was again largely expressed in the cytoplasmic fraction in control FBS-cultured cells with significantly less expression in the nuclear fraction, although immunofluorescent photomicrographs showed partial colocalization with E-cadherin, indicating localization in both the cytoplasm and in the plasma membrane (Fig. S4). DHT treatment did not affect ErbB3 localization; however, HRG did cause an increase in nuclear ErbB3, similar to that seen in LNCaP cells. Again, comparable to LNCaP, cytoplasmic ErbB3 levels were greatly increased when the cells were cultured in CSS, and DHT prevented this

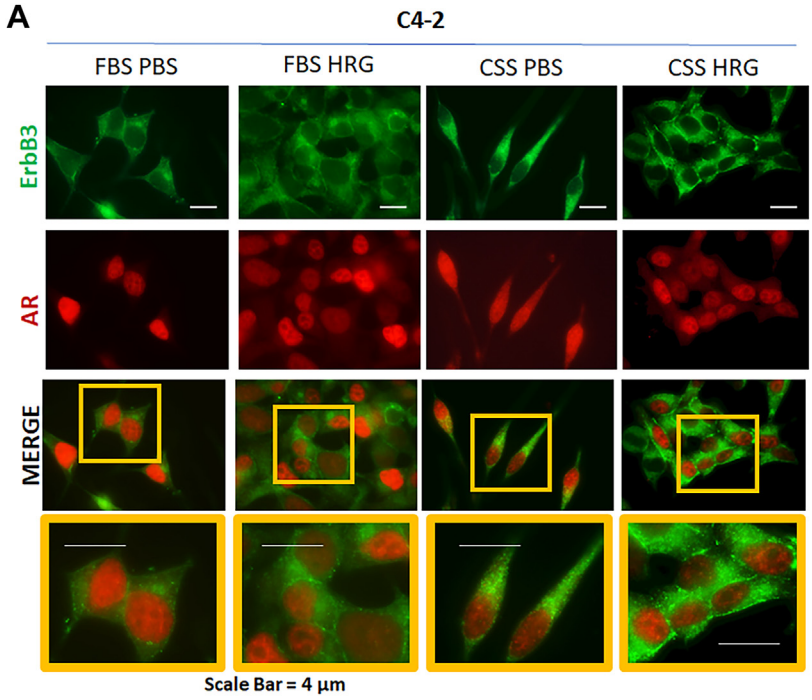

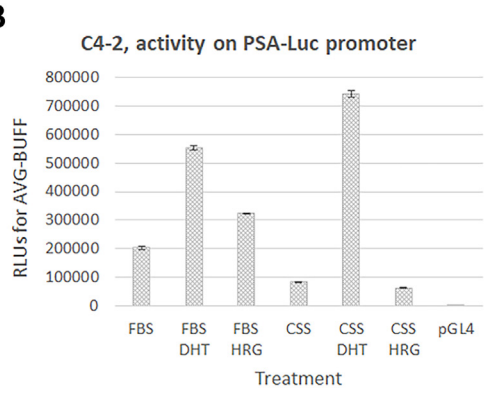

C4-2	
Treatment condition	p-value wrt FBS
FBS	
FBS DHT	6.94445E-07
FBS HRG	7.90256E-06
CSS	7.18188E-06
CSS DHT	1.91204E-07
CSS HRG	3.62855E-06

Figure 3. HRG treatment in cells cultured in FBS, but not in CSS, causes an increase in AR transcriptional activity. *A*, C4-2 cells, a subline derived from LNCaP cells, also display predominantly cytoplasmic ErbB3 whose levels increase with HRG but not DHT. AR protein remains nuclear in its localization. C4-2 cells were grown on coverslips for 72 h and treated with ligands as previously described (legend, Fig. 2). The scale bars represent 4 µm. *B*, in CRPC C4-2 cells derived from LNCaP, AR transcriptional activation on a human PSA promoter appears to increase when cytoplasmic ErbB3 staining becomes fainter. HRG is unable to transcriptionally activate the AR in the absence of androgens relative to the presence of androgens. All experiments were performed in triplicate. Error bars represent SD from the mean. Table below shows statistical analysis (Student *t* test, 2-tailed, equal variance). AR, androgen receptor; CSS, charcoal-stripped serum; DHT, dihydrotestosterone; FBS, fetal bovine serum; HRG, heregulin-1β; PSA, prostate-specific antigen.

effect. As with LNCaP, HRG did not affect CSS-mediated changes in cytoplasmic ErbB3, however, increased ErbB3 nuclear translocation (Fig. 4*A*). Thus, whereas in HSPC LNCaP cells, the presence of androgens was needed for ErbB3 nuclear translocation; in CRPC 22Rv1 cells, HRG-induced ErbB3 nuclear translocation was independent of the presence of androgens. This cell line expresses very little full-length AR and is characterized by the presence of AR splice variants that lack the AR-LBD (Fig. 4*B*). These cells express PSA, which however was enhanced by DHT alone and not HRG, indicating an effect of full-length AR (see Fig. 4*B*). Unlike LNCaP cells, in 22Rv1, DHT treatment, but not HRG, suppressed Akt and ERK phosphorylation, and in CSS, but not in FBS, both Akt and ERK phosphorylation followed ErbB3 levels. We also investigated the effect of increasing doses of HRG on 22Rv1 cells. HRG had a biphasic response in these cells with 10 ng/ml

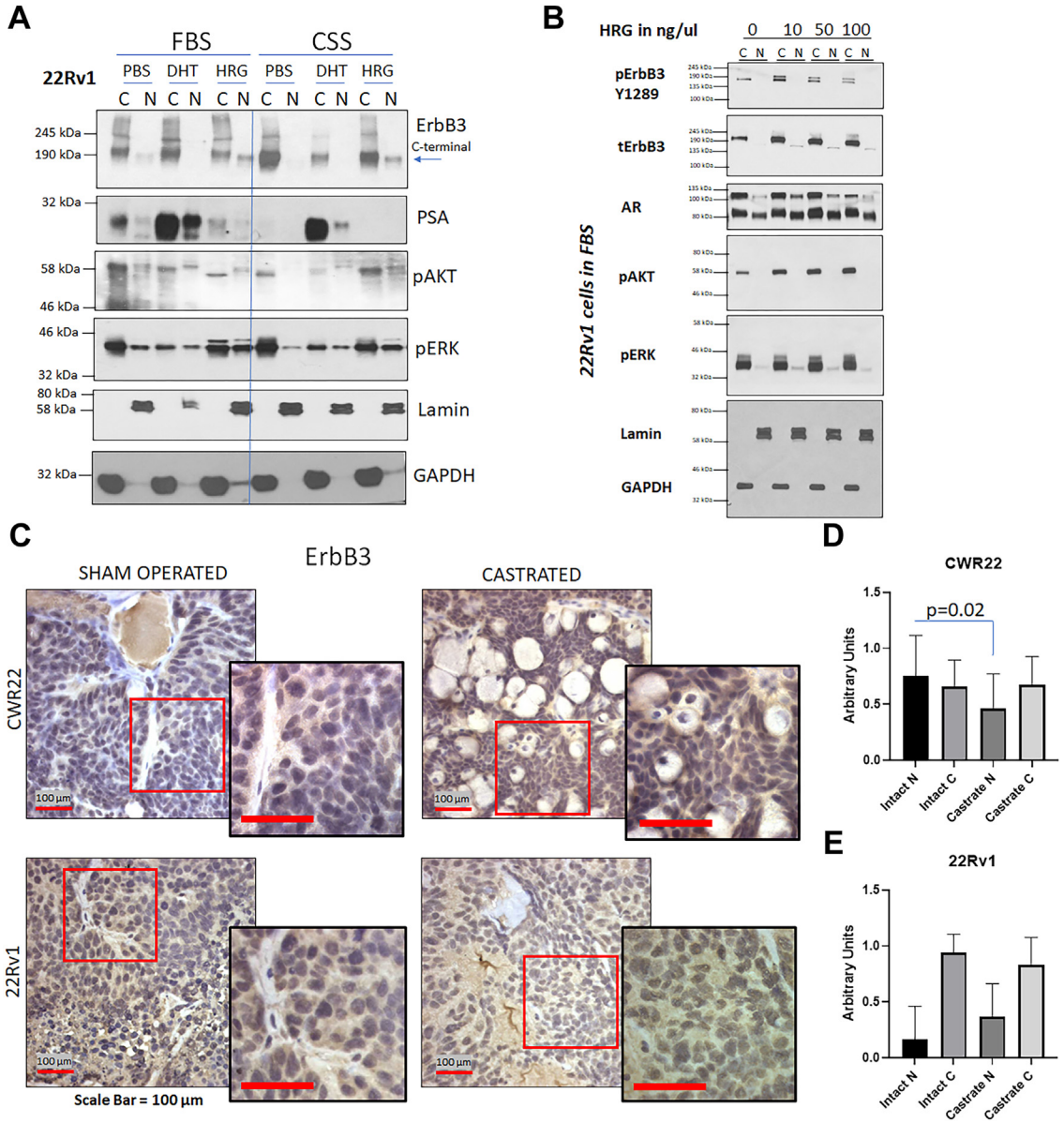

Figure 4. HRG treatment, but not AR activity, affects ErbB3 localization in CRPC 22Rv1 cells, while in parental HSPC CWR22 tumors, castration suppresses ErbB3 nuclear localization. *A*, 22Rv1 cells were cultured and treated with ligands, fractionated, and probed as previously described. Castration-resistant cells express very little nuclear ErbB3, whose levels are increased by HRG but not DHT and are unaffected by the presence of androgens. *B*, 22Rv1 cells were treated with increasing concentrations of HRG for 15 min before being collected, lysed, and analyzed by immunoblot as previously described. *C*, 4- to 5-week-old nu/nu mice were implanted (subcutaneous) with CWR22 tumor cells (AD) (n = 24) or their relapsed and androgen-resistant subline 22Rv1 cells (CRPC) (n = 24). CWR22 cells are an androgen-dependent, serially transplantable xenograft derived from a primary human prostate cancer. CWR22 tumors regress markedly after androgen withdrawal (or castration) but recur (in some animals) in 2 to 7 months. The 22Rv1 cell line was derived from this relapsed tumor, no longer responds to androgen withdrawal, and is used to model CRPC. This model behaved differently from the LNCaP xenografts and castration decreased levels of ErbB3 protein in CWR22 xenografts but appeared to have little effect in the CRPC CWR22-Rv1 xenografts. CWR22-Rv1 xenografts also appeared to display faint membrane ErbB3 staining, unlike CWR22 xenografts where ErbB3 was largely cytoplasmic. *D* and *E*, when quantified in CWR22 (*D*) and 22Rv1 tumor(*E*), these differences were found to be significant only in the former ($p < 0.05$). AR, androgen receptor; C, cytoplasmic; CRPC, castration-resistant prostate cancer; DHT, dihydrotestosterone; HRG, heregulin-1β; HSPC, hormone-sensitive prostate cancer; N, nuclear.

inducing a strong phosphorylation of ErbB3 that was suppressed at higher concentrations (Fig. 4*B*). The nuclear ErbB3 band was however observed at all doses, as was phospho-ERK.

To determine whether castration-induced ErbB3 translocation is also observed *in vivo*, we tested its validity in the HSPC, serially transplantable tumor line CWR22 along with its CRPC derivative 22Rv1. Four- to five-week-old nu/nu mice were subcutaneously implanted with CWR22 (n = 12) or 22Rv1 tumors (n = 12). In each group, mice were then either left intact (sham operated) (n = 6/line) or castrated (n = 6/line). Mice were euthanized when tumor size exceeded 150 mm^3 or at the end of the experiment. Tumors collected were formalin-fixed and paraffin-embedded (FFPE) for immunohistochemistry, and the FFPE tumors were sectioned and stained for ErbB3 (Fig. 4*C*). Staining was quantitated as described (29), and quantification for CWR22 (Fig. 4*D*) and 22Rv1 (Fig. 4*E*) were reported. 22Rv1 tumors expressed less nuclear ErbB3 (and a higher proportion of cytoplasmic ErbB3) compared to CWR22 (Fig. 4*C*). Castration decreased the staining intensity of nuclear ErbB3 in CWR22 (p = 0.02) but not 22Rv1 tumors, while cytoplasmic ErbB3 was not affected in either (Fig. 4*C*). Castration-induced decrease in nuclear ErbB3 had also been noted in LNCaP cells; hence it is likely that this is a characteristic of HSPC cells. Overall, our results indicate that while HRG translocates ErbB3 to the nucleus only in the presence of androgens in HSPC cells, HRG-induced ErbB3 nuclear translocation was androgen-independent in CRPC; similarly, castration prevented ErbB3 nuclear translocation in HSPC but not in CRPC.

ErbB3 nuclear localization by HRG requires the presence of the AR and AR signaling

We investigated whether increased ErbB3 expression by HRG and/or CSS culture required the expression of the AR. AR-null PC3 cells that also lack PTEN expression were cultured under the same conditions as above and under control conditions, displayed mostly cytoplasmic and little nuclear ErbB3 and displayed minimal alteration in ErbB3 localization with DHT either in FBS or CSS (Fig. 5*A*, left panel). When these cells were engineered to stably express full-length, WT AR (PC3-wt-AR), the regulation of ErbB3 localization seen in AR-positive cells was restored—full-length ErbB3 was now increased with HRG as did ErbB3 phosphorylation. Culture in CSS sharply increased ErbB3 phosphorylation and expression; however, supplementation with DHT did not prevent this increase (Fig. 5*A*, right panel) (densitometry analysis of nuclear and cytoplasmic ErbB3 and AR levels reported in Fig. 5, *B*–*D*). Similar to 22Rv1, HRG induced ErbB3 nuclear translocation even in CSS-cultured cells, while DHT, but not HRG, suppressed Akt phosphorylation. AR localization and levels were largely unchanged by CSS culture or with DHT or HRG treatment in PC3-wt-AR cells (Fig. 5*A* right panel). However, PC3-wt-AR cells displayed AR transcriptional activity on a PSA promoter ($p < 0.01$, Fig. 5*E*) that was lower in androgen-containing media (FBS) but increased by DHT as well as HRG in androgen-depleted media (CSS) (Fig. 5*E*, $p < 0.01$), reflecting the enhanced sensitivity of PC-3-wt-AR cells to androgens, causing the suppression of AR transcriptional activity at high levels of androgens (30). To illustrate this point, we overexpressed wt-AR in LNCaP cells that normally express a mutant AR (T877A). Despite the presence of the mutant AR, overexpression of wt-AR in LNCaP cells suppressed AR transcriptional activity on a PSA promoter. This effect demonstrates the biphasic effect of androgens in AR-positive PCa cells (activating in small amounts, inactivating when excessive). As an illustration of this effect, HRG stimulation in these cells suppressed AR activity further (Fig. S5).

By immunofluorescent microscopy, ErbB3 appeared to be both cytoplasmic and nuclear in PC3 cells (Fig. 5*F*). In contrast, ErbB3 was less nuclear and more cytoplasmic in PC3-wt-AR cells (Fig. 5*G*). ErbB3 protein was increased when the cells were cocultured with HRG and this correlated with an increase in Y1289 and pAKT, indicating the activation of that RTK (Fig. 5*A*, right panel). AR was seen in both the nucleus and the cytoplasm. These results supported the hypothesis that ErbB3 nuclear localization requires the presence of the AR and also indicate that PC-3-wt-AR cells are likely CRPC despite the expression of AR.

HRG binding to ErbB3 enables its nuclear localization, whereas AR expression keeps it in the cytoplasm

We also investigated the effects of AR expression on ErbB3 localization. In LNCaP cells, endogenous AR and ErbB3 proteins were silenced using sequence-specific siRNA (Fig. 6*A*). As before, in control cells, AR was mostly nuclear and ErbB3 was mostly cytoplasmic, and without further stimulation, AR knockdown decreased cytoplasmic ErbB3 levels, in support of patient data in Figure 1*D*, showing positive correlation between ErbB3 and AR. In support of above observation that HRG stimulates AR transcriptional activity (Fig. 3*B*), ErbB3 knockdown translocated AR from the nucleus to the cytoplasm, indicative of its inactivation. Since HRG activation of ErbB3 promotes its nuclear translocation and ErbB3 is needed for AR transcriptional activity, this suggests that HRG activation of ErbB3 nuclear localization promotes AR nuclear translocation and thereby enhances its transcriptional activity.

As before, DHT treatment increased cytoplasmic AR but did not affect ErbB3 levels (Fig. 6*A*). AR knockdown in the presence of DHT increased nuclear ErbB3, whereas ErbB3 knockdown prevented DHT-induced AR translocation. Strikingly, upon AR knockdown, HRG treatment increased nuclear ErbB3 (densitometry analysis of nuclear and cytoplasmic ErbB3 and AR levels reported in Fig. 6, *B* and *C*). PSA levels decreased when the AR was silenced but were unaffected by ErbB3 silencing. These results are supported by reporter gene assay showing the inability of DHT to rescue AR transcriptional activity on a PSA promoter when AR was knocked down (Fig. 6*D*). AKT phosphorylation was stimulated by HRG, but not DHT, and conversely decreased when ErbB3, but not AR, was silenced, indicating that it was strongly regulated by ErbB3 in LNCaP cells. Taken together, these results indicate that nuclear ErbB3 expression is stimulated by HRG in the

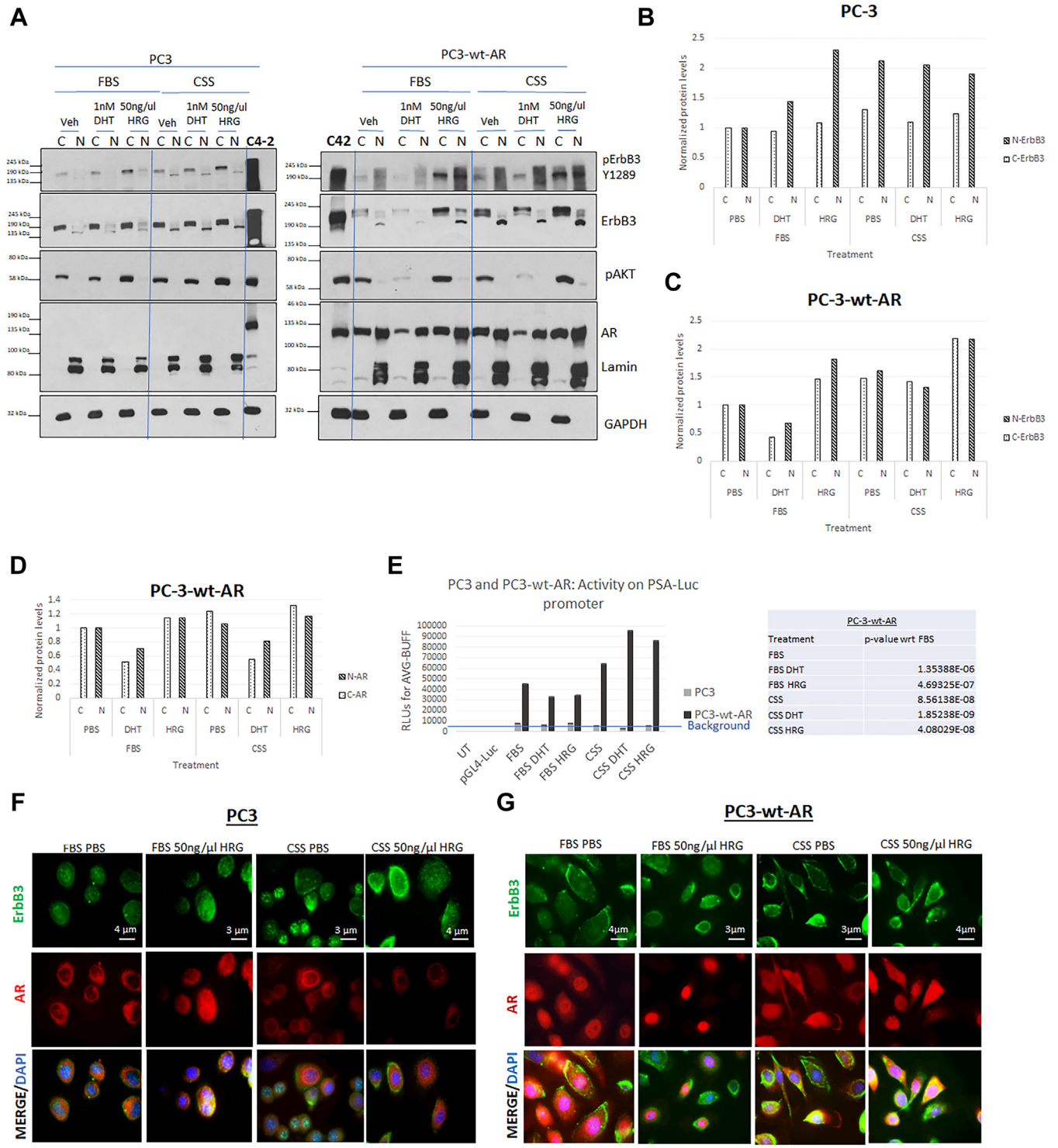

Figure 5. AR introduction in AR-null castration-resistant prostate cells restores regulation of ErbB3 localization and downstream signaling. *A*, AR-null PC3 cells ("PC3") and PC3 cells stably transfected with full-length WT AR ("PC3-wt-AR") were cultured, treated, and fractionated as previously described. ErbB3 levels and localization are unaltered in PC3 cells but increase in response to HRG in PC3-wt-AR cells. *B*, quantitation of ErbB3 bands in PC-3 cells in the nucleus (N-ErbB3) and the cytoplasm (C-ErbB3) *C*, quantitation of ErbB3 bands in PC-3-wt-AR in the nucleus (N-ErbB3) and the cytoplasm (C-ErbB3). *D*, quantitation of AR bands in PC-3-wt-AR cells in the nucleus (N-ErbB3) and the cytoplasm (C-ErbB3) using Image (*E*) PC3-wt-AR cells possess greater transcriptional activity than PC3 cells, and this transcriptional activity remains elevated in the absence of androgens in PC3-wt-AR cells but not in PC3 cells. Luciferase assays were performed as described. All experiments were performed in triplicate. Error bars represent SD from the mean. Table shows *p*-values (Student *t* test, 2-tailed, equal variance). *F*, C-terminal ErbB3 staining (CS-12708) appears diffused throughout the cytoplasm in AR-null PC3 cells. *G*, C-terminal ErbB3 appears to be localized in the cell membrane in PC3-wt-AR cells. High-magnification microscopy was performed as previously described. AR, androgen receptor; HRG, heregulin-1β.

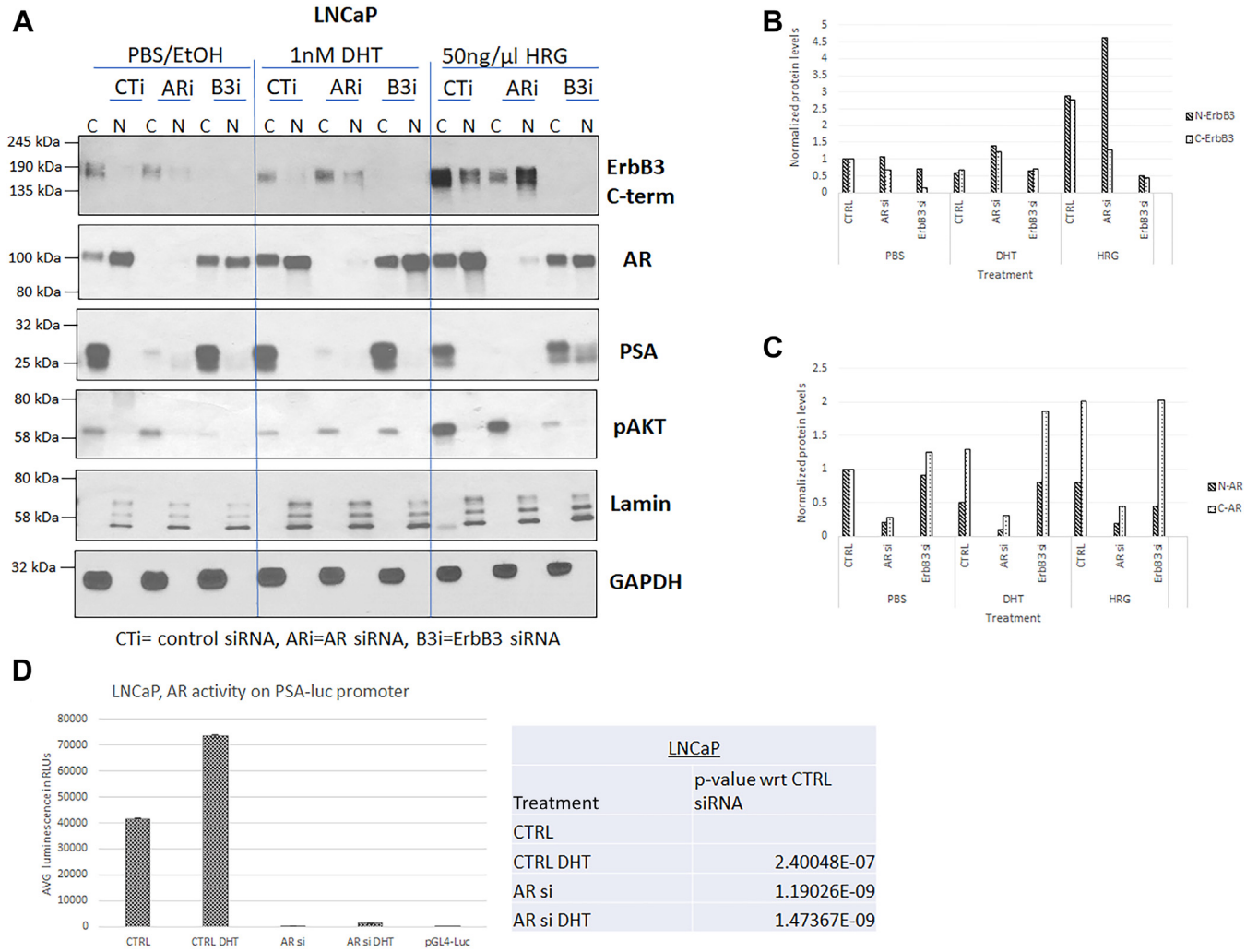

LNCaP	
Treatment	p-value wrt CTRL siRNA
CTRL	
CTRL DHT	2.40048E-07
AR si	1.19026E-09
AR si DHT	1.47367E-09

Figure 6. Divergent effect of AR transcriptional activity and AR expression on heregulin-induced ErbB3 nuclear localization. *A*, LNCaP cells were transfected with AR- or ErbB3-specific siRNA (Dharmacon) for 48 h and treated with ligands for 24 h prior to collection. Enzalutamide (Enz) is an FDA-approved AR inhibitor and was used to dissolve in 100% dimethyl sulfoxide. AR knockdown but not ErbB3 knockdown decreased PSA protein. AR knockdown increased cytoplasmic ErbB3, and ErbB3 knockdown increased cytoplasmic AR. *B*, quantitation of ErbB3 bands and (*C*) AR bands from (*A*) in the nucleus (N-ErbB3) and the cytoplasm (C-ErbB3). *D*, AR silencing decreases AR transcriptional activity on a human PSA promoter and this cannot be rescued by DHT or HRG. Luciferase assays were performed as described in detail in the legend for Figure 2. Table alongside shows relevant *p*-values. AR, androgen receptor; DHT, dihydrotestosterone; HRG, heregulin-1β; PSA, prostate-specific antigen.

presence of AR transcriptional activity but increases greatly when AR protein expression decreases. This supports the observation above that AR expression and ligand binding have opposing effects on ErbB3 localization, suggesting that while ErbB3 nuclear import is dependent on ligand-dependent AR transcriptional activity, it is likely that ErbB3 export from the nucleus is dependent on AR expression or ligand-independent AR function.

ErbB3 ligand binding is important for AR transcriptional activity, while the kinase domain is important for cell viability and Akt phosphorylation

Next, we investigated whether ErbB3 signaling is regulated by HRG binding (at its N-terminal end) or its kinase activity (at its C-terminal end). To determine whether the cytoplasmic tail plays any role in ErbB3 localization or its effect on AR, we constructed a mutant ErbB3 plasmid lacking three major phosphorylation sites (Y1222A, Y1289A, and Y1328A) ("mErbB3") (Fig. 7*A*). Hormone-sensitive LNCaP cells were transiently transfected with plasmids expressing full-length, wt AR, wt-ErbB3, or mutant ErbB3 and cultured in FBS media with or without DHT or HRG (Fig. 7*B*). AR overexpression (which increased AR expression 2-fold) did not alter ErbB3 localization in these cells; overexpression of wt and mutant ErbB3 (which increased ErbB3 levels 3- and 5-fold, respectively) caused accumulation of the RTK in the cytoplasmic fraction. DHT treatment also caused an increase in cytoplasmic ErbB3, as did treatment with HRG (Fig. 7*B*). There was no further change in ErbB3 localization upon overexpression of wt or mutant ErbB3.

In empty vector, vehicle (PBS)-treated cells, AR was nuclear, and its location was not affected when AR was overexpressed, but overexpression of mutant or wt ErB3 caused partial AR translocation to the nucleus. DHT treatment increased AR levels, and AR overexpression also enabled its partial

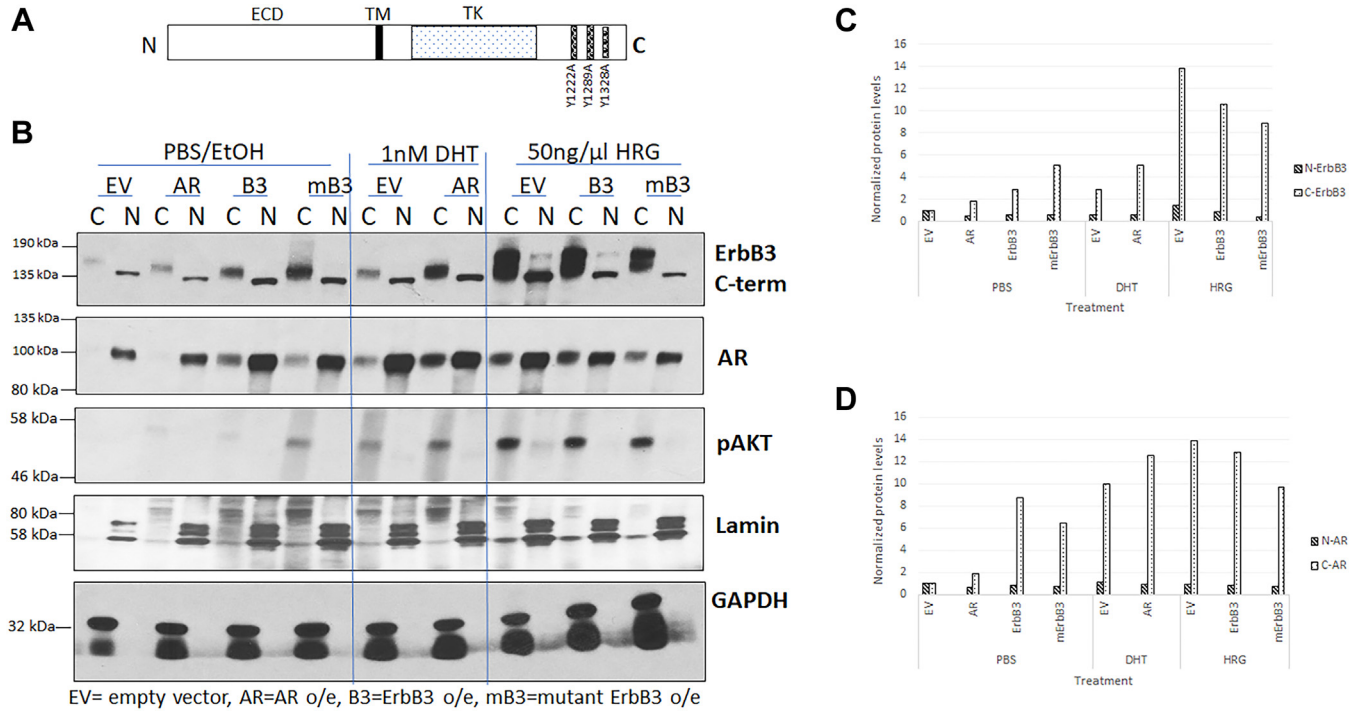

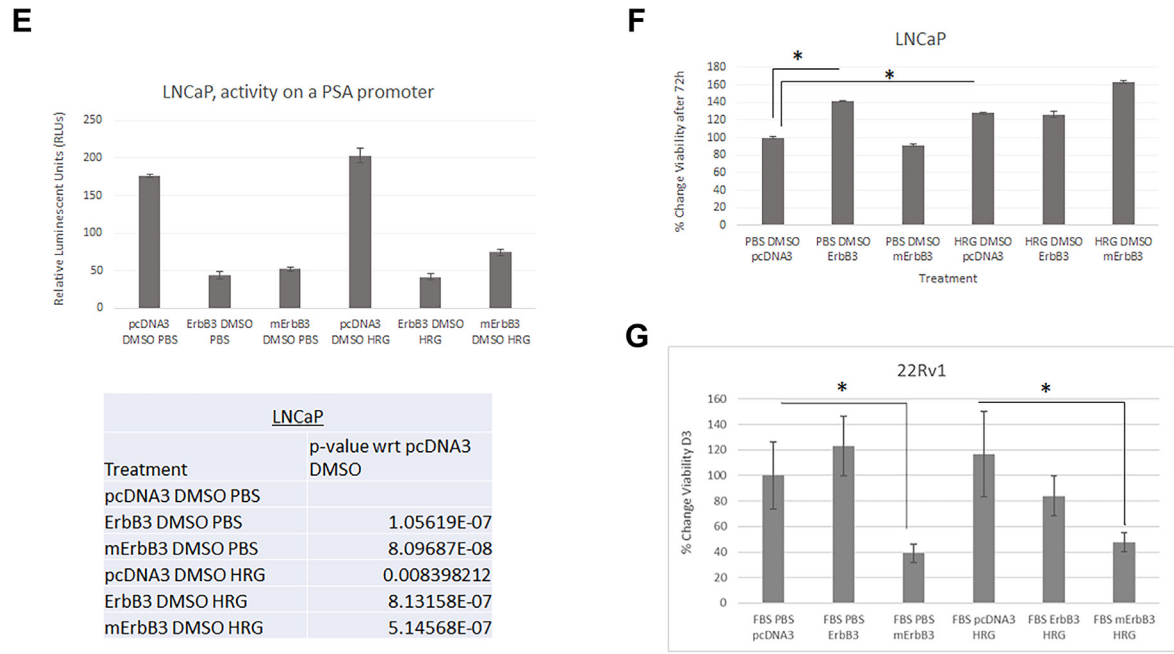

LNCaP	
Treatment	p-value wrt pcDNA3 DMSO
pcDNA3 DMSO PBS	
ErbB3 DMSO PBS	1.05619E-07
mErbB3 DMSO PBS	8.09687E-08
pcDNA3 DMSO HRG	0.008398212
ErbB3 DMSO HRG	8.13158E-07
mErbB3 DMSO HRG	5.14568E-07

Figure 7. Differential effects of AR transcriptional activity and AR expression on heregulin-induced ErbB3 and mutant ErbB3 nuclear localization. *A*, schematic of full-length ErbB3 showing mutations created on known phosphorylation sites (*black*). *B*, LNCaP cells were transfected with full-length, WT AR ("AR"), ErbB3 ("B3"), or mutated ErbB3 ("mB3" or "mErbB3") plasmids housed in a pcDNA3 ("EV") construct. Cells were transfected for 48 h and treated with ligands (1 nM DHT or 50 ng/µl HRG) for 24 h prior to collection. Lysates were separated into cytoplasmic and nuclear fractions as previously described and probed with the appropriate antibodies. *C*, quantitation of ErbB3 bands and (*D*) AR bands from (*B*) in the nucleus (N-ErbB3) and the cytoplasm (C-ErbB3). *E*, the transcriptional activity of the AR was assayed using a PSA luciferase construct in cells that had been transfected with ErbB3 or mB3 plasmids and treated with ligands as previously detailed. HRG was unable to rescue the decreased AR transcriptional activity that resulted from ErbB3 transfection. AR transcriptional activity was modestly increased by the transfection of mutated ErbB3 as compared to WT ErbB3. Readings represent the average of experiments carried out in triplicate, and error bars depict SD. Cell viability is (*F*) increased in LNCaP cells by transfection of full-length, WT ErbB3 but (*G*) decreased by mutated ErbB3 in 22Rv1 cells. All experiments were performed in triplicate. Error bars indicate SD. * indicates $p < 0.05$. AR, androgen receptor; DHT, dihydrotestosterone; ECD, extracellular domain; EV, empty vector; HRG, heregulin-1β; TK, tyrosine kinase domain; TM, transmembrane domain; PSA, prostate-specific antigen.

cytoplasmic translocation. As before, HRG treatment increased nuclear AR, and this effect was not altered when wt or mutant ErbB3 was expressed (Fig. 7*B*). The mutant ErbB3 increased Akt phosphorylation as did DHT treatment and this effect was enhanced by HRG; however, there was no difference between the effects of wt and mutant ErbB3 (densitometry analysis of nuclear and cytoplasmic ErbB3 and AR levels reported in Fig. 7, *C* and *D*). Thus, it appears that ErbB3 kinase activity is not required for AR localization in LNCaP cells. Loss of ErbB3 kinase domain, however, resulted in higher Akt phosphorylation than WT ErbB3 in unstimulated LNCaP cells, suggesting that in the absence of ligand binding, the kinase activity of ErbB3 actively suppresses downstream signaling. HRG binding, on the other hand, stimulated Akt phosphorylation, and these effects were unaltered by kinase domain inactivation.

In further evidence of the biphasic effect of AR expression on its transcriptional activity, ErbB3 overexpression in unstimulated LNCaP cells (which was mostly cytoplasmic) significantly increased AR nuclear translocation, which then suppressed AR transcriptional activity on a PSA promoter (Fig. 7*E*). This effect was unchanged by mErbB3 ($p < 0.01$), indicating uninvolvement of ErbB3 kinase activity in this process. HRG stimulation of empty vector cells did not greatly affect this process. However, AR transcriptional activity was increased 2-fold when mErbB3 was expressed in LNCaP in the presence of HRG ($p < 0.01$), which caused ErbB3 nuclear localization. Our results suggest that cytoplasmic ErbB3 suppresses AR transcriptional activity, while nuclear ErbB3 promotes it.

Finally, we investigated the effect of ErbB3 kinase activity *versus* ligand binding on cell viability. As we had previously shown, ErbB3 overexpression increased cell viability (22); this effect was prevented by mErbB3 (Fig. 7*F*). These effects were further enhanced in 22Rv1 cells; here, while wt ErbB3 did not cause a significant change in viability, mutant ErbB3 actively suppressed it (Fig. 7*G*). This raises the interesting possibility that the tyrosine phosphorylation sites are required for cell viability. This may be indicative of compensatory signaling by other ErbB family members after they have dimerized with mErbB3 (since ErbB receptors must dimerize to constitute a functionally active unit). Taken together, these results showed that the cytoplasmic tail of ErbB3, and specific tyrosine phosphorylation sites within it, were important for cell viability and played a greater role in modulating cytoplasmic ErbB3 signaling that activates Akt phosphorylation.

Discussion

In this study, we investigated the regulatory relationship between ErbB3 and the AR in HSPC *versus* CRPC cells. In agreement with existing reports (22), we observed that nuclear ErbB3 was increased in prostate tumor *versus* nontumor tissue. Examination of human PCa samples showed that cytoplasmic ErbB3, but not nuclear ErbB3, positively correlated with AR expression and negatively with its transcriptional activity. Previous reports have shown that androgen withdrawal, which suppresses AR transcriptional activity, causes an increase in AR expression (31). It is likely that a decrease in AR transcriptional activity, which increases AR expression, also causes an increase in ErbB3 levels, thereby causing this discrepancy in the relation between AR expression and its transcriptional activity (Fig. 8*A*). This is clearly shown in LNCaP cells, where culture in CSS increases AR and ErbB3 levels but show AR accumulation in the cytoplasm, where it is inactive. Negative correlation between AR transcriptional activity and ErbB3 levels is supported by our previous report that post-translational modifications on ErbB3 by the E3 ubiquitin ligase Nrdp1, which is an AR-regulated gene, caused an increase in ErbB3 levels when AR is suppressed (22). Others have shown similar effects using alternate mechanisms (32). In the present study, the increase in ErbB3 levels could be due to increased *do novo* synthesis of ErbB3 or a decrease in ErbB3 degradation (Fig. 8*B*). Further studies are needed to make that distinction.

ErbB3 is synthesized in the endoplasmic reticulum but then is transported to the plasma membrane, where it is ligand-activated and undergoes dimerization for activation. It is assumed that signal transduction to downstream targets occurs at the plasma membrane, but we see that ligand binding also allows nuclear translocation of the RTK. Our data indicates that while AR regulates the total levels of the RTK, HRG regulates its nuclear localization (Fig. 8*C*). ErbB3 contains two nuclear localization sequences (NLSs) (8) and is thought to translocate to the nucleus by binding of the NLS to importin β1 but also contains a nuclear export sequence, which helps export it back to the cytoplasm by binding to the exportin XPO1 (previously called CRM-1) (13). HRG binding enables ErbB3 nuclear localization, suggesting that ligand binding at the plasma membrane triggers activation of the NLS. However, we see that in HSPC cells, this translocation requires ligand-specific activation of the AR. Both importin β1 and XPO1 were found to contain androgen response elements, sequences on the target genes which bind to the AR-DBD (33). It is therefore likely that AR regulation of importin β1 in HSPC is a factor in HRG-induced ErbB3 nuclear localization—in the presence of androgens, the AR activates importin β1 and enables HRG-induced ErbB3 nuclear localization; in its absence, HRG is not able to stimulate this event. In contrast, in CRPC, it is likely that importin β1 is androgen-independent (*e.g.*, in 22Rv1 cells, it could be regulated by AR variants in the absence of androgen binding), hence HRG enables HRG-induced ErbB3 nuclear localization both in the presence and absence of androgens (Fig. 8*D*).

Studies show that ErbB3 nuclear localization is transient, and ErbB3 is then acted on by XPO1, which exports ErbB3 back to the cytoplasm (13). It is thought that AR acts as a scaffold for XPO1 (34); hence, in the absence of AR protein, XPO1 is not able to scurry ErbB3 back into the cytoplasm. This report is in support of our results in human tissues, showing that the expression of AR positively correlates with that of cytoplasmic ErbB3. CRPC models previously reported by others showed that castration increased the levels of nuclear ErbB3 (19). In contrast, our *in vivo* studies showed that castration reduced the amount of nuclear ErbB3 in HSPC

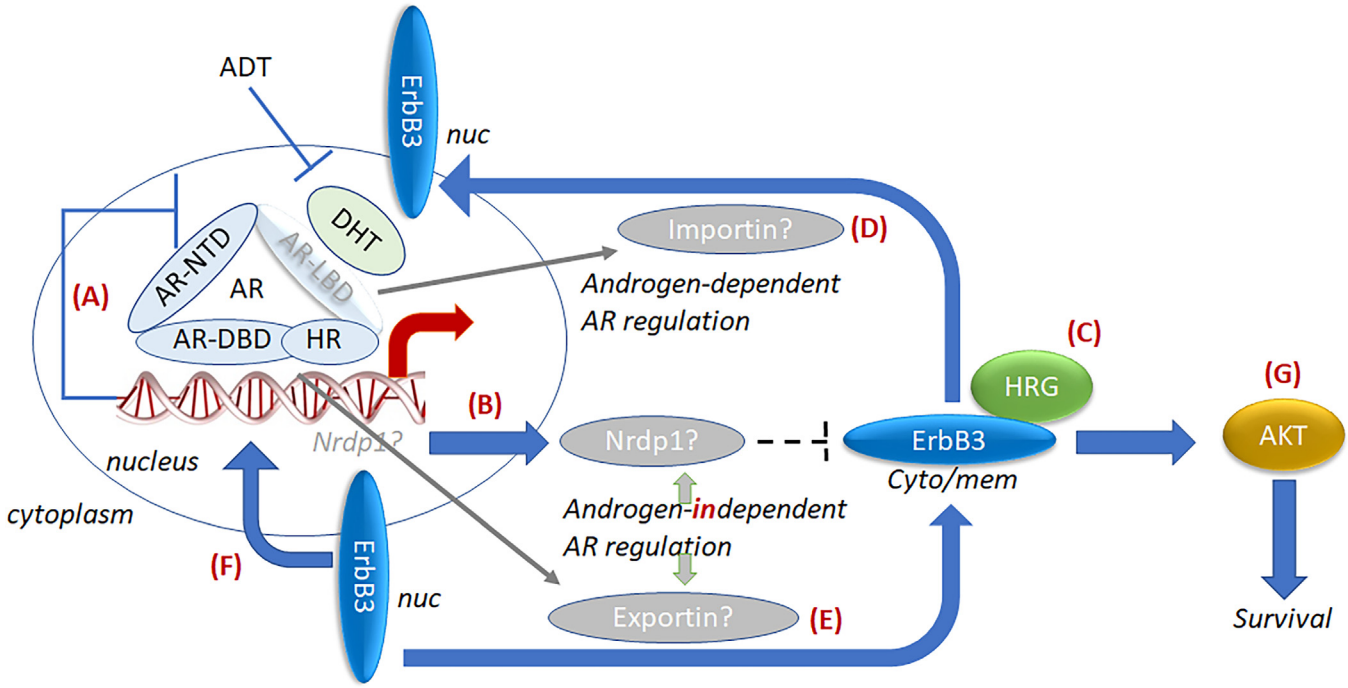

Figure 8. Schematic of proposed model of AR-ErbB3 signaling in hormone-sensitive prostate cancer *versus* castration-resistant prostate cancer. *A*, loss of AR transcriptional activity activates a negative feedback loop that results in an increase in AR expression. *B*, increased AR expression promotes the levels of ErbB3, likely by suppressing its degradation *via* regulation of its posttranslational modification as shown by us previously (22). We now see that the AR regulates ErbB3 localization through both androgen-dependent and androgen-independent pathways (AR LBD is present only in full-length AR but not in AR variants). *C*, HRG binding enables ErbB3 nuclear localization in both HSPC and CRPC cells. However, (*D*) in HSPC, androgen-dependent AR transcriptional activity is required for ErbB3 nuclear localization despite HRG stimulation, but in CRPC cells, this effect is androgen-independent. *E*, AR also regulates ErbB3 export from the nucleus to the cytoplasm in a ligand-independent manner. *F*, ErbB3 then signals to the PI3K/Akt pathway, regulating cell viability. *G*, on the other hand, HRG binding to ErbB3, which results in ErbB3 nuclear localization, is shown to result in enhanced AR transcriptional activity, indicating that nuclear ErbB3 may act as an AR coregulator. AR, androgen receptor; CRPC, castration-resistant prostate cancer; HRG, heregulin-1β; HSPC, hormone-sensitive prostate cancer; LBD, ligand-binding domain.

tumors. The latter effect can be explained by the fact that the AR also regulates the expression of XPO1 in an androgen-dependent manner in HSPC cells (33). This likely explains why, when the AR is knocked down in LNCaP cells, ErbB3 can no longer shuttle back to the cytoplasm (Fig. 8*E*). It is likely that is not the case in CRPC.

In CRPC 22Rv1 cells, culture in CSS increased the levels of cytoplasmic ErbB3, showing that in these cells, AR transcriptional activity suppressed ErbB3 levels but did not regulate its nuclear translocation. 22Rv1 cells express both full-length AR that contains a duplication of Exon 3 (which results in a larger AR protein consisting of three zinc fingers in its DBD instead of two) and that does not exist in the parental CWR22 tumors (35). In addition, 22Rv1 cells express a rare H874Y mutation in the AR-LBD (36), which also remains ligand-activated. However, 22Rv1 cell also express a number of AR variants that are transcriptionally active but are necessarily ligand-independent due to the lack of the AR-LBD (1). Given that in these cells, culture in CSS increased cytoplasmic ErbB3 levels, yet HRG-induced ErbB3 nuclear translocation remained intact; we conclude that posttranslational modifications on ErbB3 are regulated by the ligand-dependent full-length AR (which remain ligand-dependent despite its mutations), whereas ErbB3 nuclear translocation is modulated by the LBD-less AR variants. Differential gene expression has been seen in the transcriptome regulated by full-length AR *versus* AR variants lacking the AR-LBD (37, 38). It is likely that in these cells, ErbB3 nuclear localization is dependent on genes that are androgen-dependent in LNCaP cells but androgen-independent in 22Rv1; hence in the latter, HRG can induce ErbB3 nuclear localization despite the lack of androgen stimulation of the AR.

In support of these observations, in AR-null PC-3 cells, ErbB3 localization remains unaltered by changes in AR ligands, but when AR is stably transfected into these cells, HRG-induced ErbB3 nuclear translocation was observed both in CSS and in FBS, while CSS culture increased cytoplasmic ErbB3 levels, similar to that seen in 22Rv1. It may be noticed that in the PC-3-wt-AR cells, AR transcriptional activity is higher in CSS-cultured cells than in FBS-cultured cells. This phenomenon is a direct effect of the biphasic effect of androgens on the AR where at low levels of stimulation, the AR is activated, whereas upon high levels of stimulation, AR transcriptional activity is repressed (30, 39). PC-3-wt-AR cells express such high levels of AR so that this AR can be stimulated at androgen levels present in CSS. At androgen levels present in FBS, therefore, the AR is repressed and cannot transcribe downstream targets.

Knockdown of ErbB3 also affects AR expression and localization. In general, ErbB3 knockdown caused AR translocation to the cytoplasm except when the cells were also treated with DHT, in which case this effect was prevented. As AR

cytoplasmic localization indicate loss of AR transcriptional activity, its translocation to the cytoplasm by loss of ErbB3 expression suggests that ErbB3 acts as a regulator of AR transcriptional activity. In support of this hypothesis, heregulin treatment in C4-2 cells (but not in LNCaP cells), which strongly increased ErbB3 expression and ErbB3 nuclear localization, also upregulated AR transcriptional activity on a PSA promoter, suggesting the possibility that nuclear ErbB3 acts as an AR coregulator (Fig. 8*F*). Our data also demonstrate that the ErbB3 kinase domain was not involved in this effect, as mutations in the ErbB3 kinase domain did not affect AR localization. However, ErbB3 kinase activity did affect cell viability in 22Rv1 cells, although not in LNCaP. The ErbB3 kinase domain has six binding sites for the PI3K regulatory subunit p85, which transmits signals to Akt. HRG caused Akt phosphorylation in both FBS and CSS, but surprisingly, in CRPC cells, DHT suppressed Akt phosphorylation at S473. Since Akt phosphorylation was not correlated with the appearance of ErbB3 in the nucleus, we presume that ErbB3 signaling to Akt emanates from its cytoplasmic appearance (Fig. 8*G*) and enhance the impression that cytoplasmic ErbB3 suppress AR transcriptional activity, while nuclear ErbB3 enhances it.

Overall, our results indicate that HRG stimulated ErbB3 nuclear localization, but this effect requires AR transcriptional activity, which is ligand-dependent in HSPC but ligand-independent in CRPC. Thus in HSPC, but not in CRPC, androgen withdrawal prevented HRG-stimulated ErbB3 nuclear localization. However, AR expression was also needed to export ErbB3 back to the cytoplasm. In turn, nuclear ErbB3 regulated AR transcriptional activity, while cytoplasmic/membranous ErbB3 was responsible for signal transduction to downstream targets. These observations will have implications in the response of patients with PCa to ADT and support previous reports of increased association with disease progression—specifically ADT (19) and biochemical recurrence (16, 17).

Experimental procedures

Patient characteristics

All data was collected with approval from the Veterans Affairs Northern California Health Care System (VANCHCS) Institutional Review Board. Patient characteristics were retrieved from the Computerized Patient Record System of the Department of Veterans Affairs and are described elsewhere (23, 24). Sections from FFPE prostate tumors of 78 patients who underwent prostatectomy at VANCHCS were retrieved from Pathology and Laboratory Services of VANCHCS and analyzed for these studies. Tumor and nontumor areas were identified, and 60 μm core samples were extracted. Specimens were arranged in triplicate in a TMA using a Beecher Instruments Manual Tissue Arrayer.

Immunohistochemistry

TMA blocks were sectioned, and sections were heated to 60 °C and rehydrated in xylene and graded alcohols. Antigen retrieval was performed with 0.1 M citrate buffer at pH 6.0 for 20 min in a 95% water bath. Slides were allowed to cool for another 20 min, followed by sequential rinsing in PBS and 50 mM tris buffered saline with Tween 20 (TBS-T) (Tris–HCl, pH 7.6, 150 mM NaCl, Tween 20 (0.1%)). Endogenous peroxidase activity was quenched by incubation in TBS-T containing 3% hydrogen peroxide. Each incubation step was carried out at room temperature (RT) and was followed by three sequential washes (5 min each) in TBS-T. Sections were incubated in primary antibody diluted in TBS-T containing 1% ovalbumin and 1 mg/ml sodium azide (12 h), followed by incubations with biotinylated secondary antibody for 15 min, peroxidase-labeled streptavidin for 15 min (LSAB-2 Dako Corp), and diaminobenzidine and hydrogen peroxide chromogen substrate (Dako Corp) along with DAB enhancer (Signet) for 10 min. Slides were counterstained with hematoxylin and mounted. Negative controls were incubated with the same amount of antihuman polyclonal rabbit immunoglobulin G (IgG) in place of primary antibody. H&E staining was the reference for interpreting additional TMA sections. Immunohistochemistry was conducted using an ErbB3 antibody directed toward the C-terminal portion of the receptor (sc-7390, Santa Cruz Technology). The TMA slides were scored from 0 to 3 (0 = 0–25% staining, 1 = 25–50% staining, 2 = 50–75% staining, 3 = 75–100% staining), and nuclear and cytoplasmic staining were evaluated individually.

Cell culture and materials

LNCaP, 22Rv1, PC3 (ATCC), and C4-2 (MD Anderson) cells were cultured in RPMI 1640 medium with 10% FBS (Gemini Biologicals) and 1% antibiotic-antimycotic solutions (Gibco). FBS contain steroids including androgens (1 ng/ml testosterone [T]) (25) and growth factors such as epidermal growth factor, insulin-like growth factor, fibroblast growth factor, nerve growth factor, platelet-derived growth factor, etc. (26), but HRG levels have not been measured. To remove steroids and growth factors, cells were cultured in CSS that contain reduced levels of both steroids and growth factors. Cells were supplemented with 1 nM DHT or 50 ng/ml HRG. Recombinant human HRG-1β was purchased from PeproTech. DHT was obtained from Sigma-Aldrich.

Immunoblotting and band quantitation

Proteins were quantitated by bicinchonininc acid assay and ran on SDS-PAGE, then transferred on a membrane, and immunoblotted as described earlier (40, 41). The following primary antibodies were used: the rabbit mAbs anti-ErbB3 (CS-12708), phospho-ErbB3(Y1289), AR (CS-3202 and CS-5153), Lamin A/C (CS-2032), α-tubulin (CS-2125), pAKT (CS-4060), and pERK (CS-9101 were from Cell Signaling Technology. Rabbit polyclonal anti-ErbB3 antibody (sc-285) was from Santa Cruz BioTech. Mouse monoclonal anti-GAPDH (ab-8245) was from Abcam. Mouse anti-rabbit and donkey anti-mouse antibodies were obtained from Jackson ImmunoResearch Laboratories. Loading controls for cytoplasmic and nuclear fractions were GAPDH and Lamin A, respectively. Band quantitation was conducted using Image J

software (https://imagej.nih.gov/ij/download.html) (National Institutes of Health). Band intensities were normalized to that of the corresponding loading control, and resultant numbers were further normalized to the corresponding control band in the appropriate fraction. Cytoplasmic and nuclear bands were quantitated individually and normalized separately (cytoplasmic bands were normalized to cytoplasmic controls and nuclear bands were normalized to nuclear controls).

Subcellular fractionation

Cells were lysed for 15 min at RT in 500 to 900 μL of cytoplasmic lysis buffer A (10 mM Hepes pH 7.9, 10 mM KCl, 0.1 mM EDTA, 0.4% IGEPAL) with standard protease and phosphatase inhibitors. The resulting suspension was centrifuged at 16000*g* for 5 min at 4 °C, and the supernatant was transferred to a clean 1.5-ml tube and stored at −20 °C until further use. The pellet was washed thrice with 200 to 500 μL 1X PBS (Gibco, Thermo Fisher Scientific) (5 min, 16000*g*, and 4 °C) and reconstituted in ∼150 to 300 μL of 1X SDS sample buffer (10 g SDS, 4 ml 100% glycerol, 40 ml 1 M Tris–HCl pH 8.8, made up to 100 ml with doubly distilled water). The pellet was heated at 90 °C until it had completely dissolved, cooled to RT, and stored at −20 °C until further use. Proteins were quantitated and analyzed as described earlier (40).

Immunofluorescence

Cells were cultured on coverslips in 6-well plates and treated as described in the text. Upon completion, they were rinsed with PBS with 0.05% Tween-20 (PBST) and fixed with ice-cold methanol for 10 min on ice. Fixed cells were further washed three times with PBST and blocked with 5% bovine serum albumin for 1 h RT. Cells were incubated in primary antibody diluted in 1% BSA at 4 °C overnight in a humidity chamber, then again washed three times with PBST, then fluorophore-tagged secondary antibody diluted in PBST was incubated for an additional 1 h at RT in the dark. After washing thrice with cold PBST, coverslips were inverted and mounted onto uncharged glass slides with antifade mounting medium plus 4′,6-diamidino-2-phenylindole (Life Technologies) as described earlier (41). Rabbit monoclonal anti-ErbB3 (CS-12708) was from Cell Signaling Technology. Mouse monoclonal anti-AR (441) antibody was obtained from Santa Cruz Biotechnology. Mouse anti-calnexin (AB2301) was from EMD Millipore. Mouse anti-E-Cadherin (BD-610181) was from BD Biosciences . FITC- and rhodamine-tagged anti-rabbit and anti-mouse antibodies were obtained from Jackson ImmunoResearch Laboratories).

Plasmids and siRNA

PC-3 cells were stably transfected with WT AR (human pCMV-hAR, Addgene, Plasmid #89078) (PC-3-AR). For reporter gene assay, cells were transiently transfected using Lipofectamine 2000 reagent (Invitrogen), according to the manufacturer's instructions. pGL4-Luc and PSA-Luc were obtained from Promega. Specific siRNAs to AR (J-003400-06-0002) and ErbB3 (M-003127-03-0005) and nonspecific control sequences (D-001206-13-20) were obtained from Dharmacon (siGENOME SMARTPool). To create mutant ErbB3, the three desired mutations (Y1222A, Y1289A, and Y1325A) were introduced into the ErbB3 sequence (using the full-length WT ErbB3 plasmid kindly provided by Dr Kermit L. Carraway III, University of California Davis). The mutated ErbB3 sequence was synthesized with *Not1* and *Pml1* restriction sites at either end. The construct thus obtained was cut with the *Not1* and *Pml1* restriction enzymes and ligated into pcDNA3.1 (Invitrogen, Thermo Fisher Scientific). The ligation mix was transformed into Top10 competent cells (Invitrogen). The colonies were screened for the insert, inoculated for plasmid isolation, and were commercially sequence-verified.

Luciferase assay

For reporter gene assays, cells were plated in 6-well-plates and allowed to attach overnight before being transfected with 500 ng of commercially available pGL4-Luc or pGL4-hPSA-Luc constructs (Promega). For cotransfections, 2.5 μl of the appropriate siRNA or 500 ng of the appropriate DNA construct were used. After removal of the construct–lipid complexes, cells were treated with the appropriate medium and ligand conditions and allowed to incubate at 37 °C/5% CO_2 for 48 h before being collected, lysed, and analyzed for AR transcriptional activity using a commercially available kit as per manufacturer's instructions (E4550, Promega). Experiments were performed in triplicate.

Animal studies

All animal studies were conducted, and data collected with approval from the University of California Davis institutional animal care and use committee. Animal studies were performed as described previously (29). In summary, 4- to 5-week-old male Balb/c athymic Foxn1^{nu} (nu/nu) mice (Harlan Sprague Dawley, Inc) were subcutaneously implanted in the flank with suspensions of CWR22 or 22Rv1 (2.5 million cells/site) in 50% Matrigel-solubilized basement membrane (BD Biosciences) and xenografts established. When palpable tumors were observed, the animals were castrated by bilateral scrotal excision, following isoflurane anesthetization or sham-operated by opening the animals surgically, but no tissues were removed. Mice were sacrificed when tumor size exceeded 150 mm in any one dimension or at the end of the study period. Mouse tumors were fixed in 10% buffered formalin (Medical Industries) for 30 min at RT, after which the pellet was immersed in 600-μl liquefied agar at 50 to 60 °C. The agar containing the tumor was paraffin-embedded and processed based on established protocols. Tumors were then stained with rabbit polyclonal anti-ErbB3 (CS-12708; 1:100 dilution, Cell Signaling Technologies).

Statistical analysis

Due to the non-normality of the data, nonparametric statistical methods were used throughout. Median staining levels were compared between cancer and noncancer cells from the same subject using Wilcoxon signed-rank tests. Median staining levels were compared between levels of categorical

demographic characteristics using Wilcoxon rank-sum tests, in the case of demographic characteristics with two levels, or using Kruskal-Wallis tests, in the case of demographic characteristics with more than two levels. The correlations between staining levels and continuous demographic characteristics were estimated using Spearman's rho. All analyses were conducted using R, version 2.13.0 (https://cran-archive.rproject.org/bin/windows/base/old/2.13.0/) (R Development Core Team, 2011). Reporter gene experiments were analyzed using two-tailed Student's *t* test assuming equal variance, while graphs of raw data were generated using scatterplot function (Microsoft Excel).

Data availability

All data generated during this study are included in this document and/or the supporting information files.

Supporting information—This article contains supporting information.

Acknowledgments—pcDNA3 and pcDNA3-ErbB3 plasmids were kindly provided by Dr Kermit L. Carraway III, University of California, Davis, California. WT androgen receptor plasmid (pAR0) was kindly provided by Dr Albert O. Brinkman, Erasmus University, the Netherlands. Manuscript review and editing was performed by Dr Christopher A. Lucchesi, University of California, Davis and Research Service, Veterans Affairs Northern California Healthcare System, Mather, CA.

Author contributions—M. K. J., S. S., B. P. D. J., B. A. M., L. S. D. A., and N. B. investigation; M. K. J., B. A. M., L. S. D. A., and N. B. methodology; M. K. J., S. S., D. M. V., B. P. D. J., C. D., M. M., and P. M. G. formal analysis; M. K. J. and S. S. visualization; M. K. J. and P. M. G. conceptualization; M. K. J., B. A. M., and N. B. validation; M. K. J. writing-original draft; M. K. J., D. M. V., B. P. D. J., M. M., and P. M. G. writing-review and editing; M. K. J. and P. M. G. funding acquisition; P. M. G. resources; P. M. G. supervision; P. M. G. project administration; M. K. J., S. S., D. M. V., M. M., and P. M. G. data curation.

Funding and additional information—This work was supported in part by a grant from the Department of Defense (DOD) Congressionally Directed Medical Research Programs (CDMRP) Prostate Cancer Research Program (PCRP) (W81XWH-21-1-0073) to M. K. J., by Biomedical Laboratory Research & Development (BLRD) Merit Award (I01BX004423, P. M. G.) from the Department of Veterans Affairs and by Award R01CA185509 (P. M. G.) from the National Institutes of Health. We are grateful for a generous award from the University of California Comprehensive Cancer Center Support Grant (P30CA093373) for this project (P. M. G.). The content is solely the responsibility of the authors and does not necessarily represent the official views of the National Institutes of Health, the Department of Veterans Affairs or the United States Government.

Conflict of interest—The authors declare that they have no conflicts of interest with the contents of this article.

Abbreviations—The abbreviations used are: ADT, androgen deprivation therapy; AR, androgen receptor; CRPC, castration-resistant prostate cancer; CSS, charcoal-stripped serum; DBD, DNA-binding domain; DHT, dihydrotestosterone; EGFR, epidermal growth factor receptor; FBS, fetal bovine serum; FFPE, formalin-fixed and paraffin-embedded; HRG, heregulin-1β; HSPC, hormone-sensitive prostate cancer; LBD, ligand-binding domain; NLS, nuclear localization sequence; PBST, PBS with 0.05% Tween-20; PCa, prostate cancer; PSA, prostate-specific antigen; RT, room temperature; RTK, receptor tyrosine kinase; TMA, tissue microarray; VANCHCS, VA Northern California Health Care System.

References

1. Messner, E. A., Steele, T. M., Tsamouri, M. M., Hejazi, N., Gao, A. C., Mudryj, M., *et al.* (2020) The androgen receptor in prostate cancer: effect of structure, ligands and spliced variants on therapy. *Biomedicines* **8**, 422
2. Chandrasekar, T., Yang, J. C., Gao, A. C., and Evans, C. P. (2015) Mechanisms of resistance in castration-resistant prostate cancer (CRPC). *Transl Androl. Urol.* **4**, 365–380
3. Yarden, Y., and Pines, G. (2012) The ERBB network: at last, cancer therapy meets systems biology. *Nat. Rev. Cancer* **12**, 553
4. Seruga, B., Ocana, A., and Tannock, I. F. (2011) Drug resistance in metastatic castration-resistant prostate cancer. *Nat. Rev. Clin. Oncol.* **8**, 12
5. Marti, U., Burwen, S. J., Wells, A., Barker, M. E., Huling, S., Feren, A. M., *et al.* (1991) Localization of epidermal growth factor receptor in hepatocyte nuclei. *Hepatology* **13**, 15–20
6. Giri, D. K., Ali-Seyed, M., Li, L.-Y., Lee, D.-F., Ling, P., Bartholomeusz, G., *et al.* (2005) Endosomal transport of ErbB-2: mechanism for nuclear entry of the cell surface receptor. *Mol. Cell. Biol.* **25**, 11005–11018
7. Offterdinger, M., Schöfer, C., Weipoltshammer, K., and Grunt, T. W. (2002) c-erbB-3: a nuclear protein in mammary epithelial cells. *J. Cell Biol.* **157**, 929–940
8. Adilakshmi, T., Ness-Myers, J., Madrid-Aliste, C., Fiser, A., and Tapinos, N. (2011) A nuclear variant of ErbB3 receptor tyrosine kinase regulates ezrin distribution and Schwann cell myelination. *J. Neurosci.* **31**, 5106–5119
9. Carpenter, G. (2003) Nuclear localization and possible functions of receptor tyrosine kinases. *Curr. Opin. Cell Biol.* **15**, 143–148
10. Jathal, M. K., Chen, L., Mudryj, M., and Ghosh, P. M. (2011) Targeting ErbB3: the new RTK(id) on the prostate cancer block. *Immunol. Endocr. Metab. Agents Med. Chem.* **11**, 131–149
11. Lo, H., and Hung, M. (2006) Nuclear EGFR signalling network in cancers: linking EGFR pathway to cell cycle progression, nitric oxide pathway and patient survival. *Br. J. Cancer* **94**, 184
12. Xia, W., Liu, Z., Zong, R., Liu, L., Zhao, S., Bacus, S. S., *et al.* (2011) Truncated ErbB2 expressed in tumor cell nuclei contributes to acquired therapeutic resistance to ErbB2 Kinase InhibitorsTruncated, Nuclear ErbB2 and Resistance to ErbB2 TKI. *Mol. Cancer Ther.* **10**, 1367–1374
13. Reif, R., Adawy, A., Vartak, N., Schröder, J., Günther, G., Ghallab, A., *et al.* (2016) Activated ErbB3 translocates to the nucleus via Clathrin-independent endocytosis, which is associated with proliferating cells. *J. Biol. Chem.* **291**, 3837–3847
14. Kim, J., Jeong, H., Lee, Y., Kim, C., Kim, H., and Kim, A. (2013) HRG-β1-driven ErbB3 signaling induces epithelial–mesenchymal transition in breast cancer cells. *BMC cancer* **13**, 383
15. Andrique, L., Fauvin, D., El Maassarani, M., Colasson, H., Vannier, B., and Séité, P. (2012) ErbB3 80 kDa, a nuclear variant of the ErbB3 receptor, binds to the Cyclin D1 promoter to activate cell proliferation but is negatively controlled by p14 ARF. *Cell. Signal.* **24**, 1074–1085
16. Koumakpayi, I. H., Diallo, J.-S., Le Page, C., Lessard, L., Filali-Mouhim, A., Bégin, L. R., *et al.* (2007) Low nuclear ErbB3 predicts biochemical recurrence in patients with prostate cancer. *BJU Int.* **100**, 303–309
17. Koumakpayi, I. H., Diallo, J.-S., Le Page, C., Lessard, L., Gleave, M., Bégin, L. R., *et al.* (2006) Expression and nuclear localization of ErbB3 in prostate cancer. *Clin. Cancer Res.* **12**, 2730–2737

18. El Maassarani, M., Barbarin, A., Fromont, G., Kaissi, O., Lebbe, M., Vannier, B., *et al.* (2016) Integrated and functional genomics analysis validates the relevance of the nuclear variant ErbB380kDa in prostate cancer progression. *PLoS One* **11**, e0155950
19. Cheng, C.-J., Ye, X.-C., Vakar-Lopez, F., Kim, J., Tu, S.-M., Chen, D.-T., *et al.* (2007) Bone microenvironment and androgen status modulate subcellular localization of ErbB3 in prostate cancer cells. *Mol. Cancer Res.* **5**, 675–684
20. Lin, S. H., Cheng, C. J., Lee, Y. C., Ye, X., Tsai, W. W., Kim, J., *et al.* (2008) A 45-kDa ErbB3 secreted by prostate cancer cells promotes bone formation. *Oncogene* **27**, 5195–5203
21. Lee, H., Akita, R. W., Sliwkowski, M. X., and Maihle, N. J. (2001) A naturally occurring secreted human ErbB3 receptor isoform inhibits heregulin-stimulated activation of ErbB2, ErbB3, and ErbB4. *Cancer Res.* **61**, 4467–4473
22. Chen, L., Siddiqui, S., Bose, S., Mooso, B., Asuncion, A., Bedolla, R. G., *et al.* (2010) Nrdp1-mediated regulation of ErbB3 expression by the androgen receptor in androgen-dependent but not castrate-resistant prostate cancer cells. *Cancer Res.* **70**, 5994–6003
23. D'Abronzo, L. S., Bose, S., Crapuchettes, M. E., Beggs, R. E., Vinall, R. L., Tepper, C. G., *et al.* (2017) The androgen receptor is a negative regulator of eIF4E phosphorylation at S209: implications for the use of mTOR inhibitors in advanced prostate cancer. *Oncogene* **36**, 6359–6373
24. Siddiqui, S., Libertini, S. J., Lucas, C. A., Lombard, A. P., Baek, H. B., Nakagawa, R. M., *et al.* (2020) The p14ARF tumor suppressor restrains androgen receptor activity and prevents apoptosis in prostate cancer cells. *Cancer Lett.* **483**, 12–21
25. Song, W., and Khera, M. (2014) Physiological normal levels of androgen inhibit proliferation of prostate cancer cells *in vitro*. *Asian J. Androl.* **16**, 864–868
26. Lee, D. Y., Lee, S. Y., Yun, S. H., Jeong, J. W., Kim, J. H., Kim, H. W., *et al.* (2022) Review of the current research on fetal bovine serum and the development of cultured meat. *Food Sci. Anim. Resour.* **42**, 775–799
27. Savoy, R. M., Chen, L., Siddiqui, S., Melgoza, F. U., Durbin-Johnson, B., Drake, C., *et al.* (2015) Transcription of Nrdp1 by the androgen receptor is regulated by nuclear filamin A in prostate cancer. *Endocr. Relat. Cancer* **22**, 369–386
28. Wu, H. C., Hsieh, J. T., Gleave, M. E., Brown, N. M., Pathak, S., and Chung, L. W. (1994) Derivation of androgen-independent human LNCaP prostatic cancer cell sublines: role of bone stromal cells. *Int. J. Cancer* **57**, 406–412
29. Chen, L., Mooso, B. A., Jathal, M. K., Madhav, A., Johnson, S. D., van Spyk, E., *et al.* (2011) Dual EGFR/HER2 inhibition sensitizes prostate cancer cells to androgen withdrawal by suppressing ErbB3. *Clin. Cancer Res.* **17**, 6218–6228
30. de Launoit, Y., Veilleux, R., Dufour, M., Simard, J., and Labrie, F. (1991) Characteristics of the biphasic action of androgens and of the potent antiproliferative effects of the new pure antiestrogen EM-139 on cell cycle kinetic parameters in LNCaP human prostatic cancer cells. *Cancer Res.* **51**, 5165–5170
31. Labaf, M., Li, M., Ting, L., Karno, B., Zhang, S., Gao, S., *et al.* (2022) Increased AR expression in castration-resistant prostate cancer rapidly induces AR signaling reprogramming with the collaboration of EZH2. *Front. Oncol.* **12**, 1021845
32. Zhang, Y., Wang, X. W., Jelovac, D., Nakanishi, T., Yu, M. H., Akinmade, D., *et al.* (2005) The ErbB3-binding protein Ebp1 suppresses androgen receptor-mediated gene transcription and tumorigenesis of prostate cancer cells. *Proc. Natl. Acad. Sci. U. S. A.* **102**, 9890–9895
33. Wilson, S., Qi, J., and Filipp, F. V. (2016) Refinement of the androgen response element based on ChIP-Seq in androgen-insensitive and androgen-responsive prostate cancer cell lines. *Sci. Rep.* **6**, 32611
34. Schütz, S. V., Cronauer, M. V., and Rinnab, L. (2010) Inhibition of glycogen synthase kinase-3beta promotes nuclear export of the androgen receptor through a CRM1-dependent mechanism in prostate cancer cell lines. *J. Cell. Biochem.* **109**, 1192–1200
35. Tepper, C. G., Boucher, D. L., Ryan, P. E., Ma, A. H., Xia, L., Lee, L. F., *et al.* (2002) Characterization of a novel androgen receptor mutation in a relapsed CWR22 prostate cancer xenograft and cell line. *Cancer Res.* **62**, 6606–6614
36. Attardi, B. J., Burgenson, J., Hild, S. A., and Reel, J. R. (2004) Steroid hormonal regulation of growth, prostate specific antigen secretion, and transcription mediated by the mutated androgen receptor in CWR22Rv1 human prostate carcinoma cells. *Mol. Cell. Endocrinol.* **222**, 121–132
37. Krause, W. C., Shafi, A. A., Nakka, M., and Weigel, N. L. (2014) Androgen receptor and its splice variant, AR-V7, differentially regulate FOXA1 sensitive genes in LNCaP prostate cancer cells. *Int. J. Biochem. Cell Biol.* **54**, 49–59
38. Miller, K. J., Henry, I., Maylin, Z., Smith, C., Arunachalam, E., Pandha, H., *et al.* (2023) A compendium of Androgen Receptor Variant 7 target genes and their role in castration resistant prostate cancer. *Front. Oncol.* **13**, 1129140
39. Shao, C., Wang, Y., Yue, H. H., Zhang, Y. T., Shi, C. H., Liu, F., *et al.* (2007) Biphasic effect of androgens on prostate cancer cells and its correlation with androgen receptor coactivator dopa decarboxylase. *J. Androl.* **28**, 804–812
40. Mooso, B. A., Vinall, R. L., Tepper, C. G., Savoy, R. M., Cheung, J. P., Singh, S., *et al.* (2012) Enhancing the effectiveness of androgen deprivation in prostate cancer by inducing Filamin A nuclear localization. *Endocr. Relat. Cancer* **19**, 759–777
41. Jathal, M. K., Steele, T. M., Siddiqui, S., Mooso, B. A., D'Abronzo, L. S., Drake, C. M., *et al.* (2019) Dacomitinib, but not lapatinib, suppressed progression in castration-resistant prostate cancer models by preventing HER2 increase. *Br. J. Cancer* **121**, 237–248